Targeting the Extrinsic Pathway of Hepatocyte Apoptosis Promotes Clearance of *Plasmodium* Liver Infection

Graphical Abstract

Created with BioRender

Highlights

- cIAPs are upregulated during *Plasmodium* liver infection

- Inactivation of cIAPs preferentially kills liver-stage malaria parasites

- IAP antagonists induce extrinsic apoptosis of infected hepatocytes and promote immunity

- Targeting extrinsic apoptosis signaling could be a way to manage malaria infections
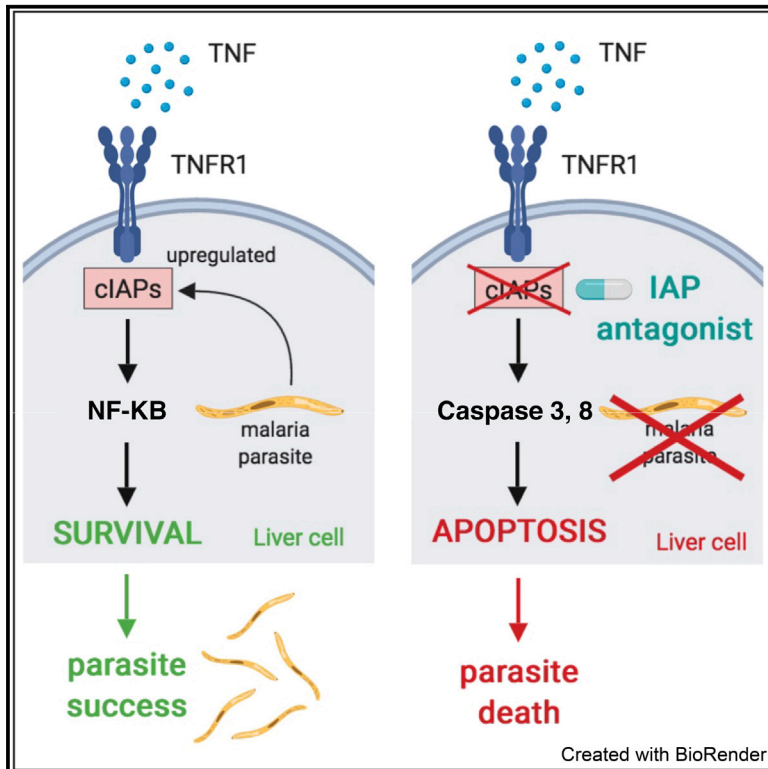
Authors

Gregor Ebert, Sash Lopaticki,
Matthew T. O'Neill, ..., John Silke,
Marc Pellegrini, Justin A. Boddey

Correspondence

pellegrini@wehi.edu.au (M.P.),
boddey@wehi.edu.au (J.A.B.)

In Brief

Ebert et al. reveal that cellular inhibitor of apoptosis proteins (cIAPs) are upregulated in the liver during *Plasmodium* infection. Inactivation of cIAPs kills *Plasmodium* liver stages via TNF-mediated apoptosis of infected hepatocytes, affecting disease and promoting immunity. Targeting extrinsic apoptosis of infected host cells may be an antimalarial avenue.

CellPress

Targeting the Extrinsic Pathway of Hepatocyte Apoptosis Promotes Clearance of *Plasmodium* Liver Infection

Gregor Ebert,[1,2] Sash Lopaticki,[1] Matthew T. O'Neill,[1] Ryan W.J. Steel,[1,2] Marcel Doerflinger,[1,2] Pravin Rajasekaran,[1,2] Annie S.P. Yang,[1,2] Sara Erickson,[1,2] Lisa Ioannidis,[1,2] Philip Arandjelovic,[1,2] Liana Mackiewicz,[1] Cody Allison,[1,2] John Silke,[1,2] Marc Pellegrini,[1,2,*] and Justin A. Boddey[1,2,3,*]
[1]The Walter and Eliza Hall Institute of Medical Research, Parkville, VIC, Australia
[2]Department of Medical Biology, The University of Melbourne, Parkville, VIC, Australia
[3]Lead Contact
*Correspondence: pellegrini@wehi.edu.au (M.P.), boddey@wehi.edu.au (J.A.B.)
https://doi.org/10.1016/j.celrep.2020.03.032

SUMMARY

***Plasmodium* sporozoites infect the liver and develop into exoerythrocytic merozoites that initiate blood-stage disease. The hepatocyte molecular pathways that permit or abrogate parasite replication and merozoite formation have not been thoroughly explored, and a deeper understanding may identify therapeutic strategies to mitigate malaria. Cellular inhibitor of apoptosis (cIAP) proteins regulate cell survival and are co-opted by intracellular pathogens to support development. Here, we show that cIAP1 levels are upregulated during *Plasmodium* liver infection and that genetic or pharmacological targeting of cIAPs using clinical-stage antagonists preferentially kills infected hepatocytes and promotes immunity. Using gene-targeted mice, the mechanism was defined as TNF-TNFR1-mediated apoptosis via caspases 3 and 8 to clear parasites. This study reveals the importance of cIAPs to *Plasmodium* infection and demonstrates that host-directed antimalarial drugs can eliminate liver parasites and induce immunity while likely providing a high barrier to resistance in the parasite.**

INTRODUCTION

Plasmodium parasites are estimated to infect more than 200 million people each year and cause 619,000 malaria-related deaths annually (Weiss et al., 2019). The greatest morbidity and mortality from malaria occur in children under the age of 5 years. Malaria parasites are transmitted through the bite of infected female *Anopheles* mosquitoes that inoculate sporozoites into the skin. Sporozoites home to the liver, where they infect hepatocytes. The hepatic stage of *Plasmodium* infection is critical for the production and release of merozoites that infect erythrocytes and cause symptomatic malaria (Vaughan and Kappe, 2017). Dissection of the relationship between parasite and human host has been strongly focused on the erythrocytic stage and has led to major epidemiological and mechanistic advance-

ments, including the identification of numerous red cell disorders that protect against malaria (Taylor and Fairhurst, 2014). Examination of the hepatic stage has also been an important research focus. However, the hepatic factors that perpetuate or restrict infection are still not fully defined.

The evolution of human genetic mutations that confer erythrocyte resistance to malaria parasite infection suggests that manipulating host factors may represent a powerful approach to manage or treat *Plasmodium* infections, including during the liver stage (Douglass et al., 2015; Kain et al., 2020; Kaushansky et al., 2013; Raphemot et al., 2019). Because transition through the liver is a crucial bottleneck for establishing malaria, we focused on dissecting molecular signaling events within parasite-infected hepatocytes required to sustain liver-stage infection with a view of targeting them therapeutically.

Host cell survival and cell death signaling pathways have been implicated in the control and pathogenesis of many infectious diseases (Lamkanfi and Dixit, 2010; Yatim and Albert, 2011; Zitvogel et al., 2010), and *Plasmodium* liver-stage parasites are known to subvert hepatocyte apoptosis signaling in order to survive (Albuquerque et al., 2009; Leirião et al., 2005; van de Sand et al., 2005). Apoptosis is a non-lytic form of cell death that helps protect the host by destroying the replicative niche of intracellular pathogens and the pathogen itself (Ebert et al., 2015a). Therefore, to persist and replicate, intracellular pathogens must passively or actively avoid host cell apoptosis. One form of apoptosis is driven by autocrine and paracrine production of death ligands, including tumor necrosis factor (TNF) (Ashkenazi and Dixit, 1998; Micheau and Tschopp, 2003). TNF is produced by pathogen-infected cells and immune, stromal, and epithelial cells under various physiological and pathological conditions. Generally, the apoptotic properties of TNF are constrained by inhibitor of apoptosis proteins (IAPs). IAPs are a family of proteins including cellular IAP1 (cIAP1), cIAP2, and X-linked IAP (XIAP), which function as ubiquitin E3 ligases via their RING domain. cIAP1 and cIAP2 are known for their ability to inhibit caspase-8-induced apoptosis and tightly regulate TNF-mediated cell survival signaling (Lalaoui and Vaux, 2018).

When TNF binds its cognate death receptor TNFR1, the cIAPs are recruited to the signaling complex, and they cause activation of NF-κB and MAPKs, production of inflammatory cytokines, and cell survival (Bertrand et al., 2008; Mahoney et al., 2008;

Varfolomeev et al., 2008). However, if cIAPs are antagonized, TNF ligation to TNFR1 causes the activation of caspase-8 to initiate the apoptotic program (Varfolomeev et al., 2007; Vince et al., 2007). Previously, this molecular machinery has been harnessed to promote the clearance of hepatitis B virus infection in the liver by genetically and pharmacologically targeting cIAP1 and cIAP2 (Ebert et al., 2015a, 2015b).

Here, we investigated whether cIAPs could be a nexus for abrogating *Plasmodium* liver infection. Using conditionally gene-targeted animals and pharmacological approaches, we found that cIAPs were required to preserve liver-stage parasites that give rise to blood-stage malaria infections *in vivo*. Infected mice treated with clinical-stage IAP antagonists had augmented immunity to liver-stage infection upon challenge with sporozoites. Together, these data define an important role for cIAPs in maintaining the survival and development of liver-stage parasites within hepatocytes and provide therapeutic insights that may be exploited to promote immunity to liver-stage infection in malaria-endemic areas.

RESULTS

cIAPs Sustain *Plasmodium* Liver Infection

To determine whether the pro-survival cIAPs are essential for liver-stage malaria parasite growth, we infected mice with *P. berghei* sporozoites and assessed expression of IAPs (XIAP and cIAP1) in mouse livers by immunoblotting. XIAP levels remained unchanged (Figure 1A; Figure S1A), but we observed an approximately 50% increase in cIAP1 levels in livers of infected compared with uninfected mice (Figure 1A; Figure S1B). Protein levels of cIAP2 could not be assessed, because of the lack of reliable mouse cIAP2-specific antibodies. This suggested that cIAPs may be important for parasite survival and growth during the liver stage. To investigate this hypothesis, we inoculated sporozoites into mice that contained $clap1^{\Delta Hep/\Delta Hep}$ $clap2^{-/-}$ compound mutations, which are deficient in cIAP2 and specifically lack cIAP1 in hepatocytes, and measured the kinetics of parasite infection. Mice deficient in cIAPs had comparable parasite burdens in the liver soon after infection (6 h) compared with wild-type (WT) animals, indicating that the loss of cIAPs did not interfere with initiation of infection. However, $clap1^{\Delta Hep/\Delta Hep}$ $clap2^{-/-}$ mice showed a dramatic reduction in parasite liver load at 20 and 44 h post-infection (Figure 1B). Consistent with this >95% reduction in liver burden, a 1 to 2 day delay in the pre-patent period (the time for liver-stage parasites to establish blood-stage infection) was observed (Figure 1C). One $clap1^{\Delta Hep/\Delta Hep}$ $clap2^{-/-}$ mouse did not develop blood-stage malaria during the observation period (Figure 1C). Loss of cIAPs was also associated with improved survival of infected mice (Figure 1D). Therefore, cIAPs play an important role in sustaining the development of *P. berghei* exoerythrocytic forms (EEFs) within the liver, consistent with the upregulation of cIAP1 during liver-stage infection. During the course of liver-stage infection, we did not detect any major perturbations in detectable serum cytokine levels in experimental or control infected animals (Figures S1C–S1G), although there was a significant albeit small increase in serum TNF levels in mutant mice compared with controls following infection (Figure 1E). There was also an increase in TNF receptor 1 (TNFR) protein levels in the

livers of $clap1^{\Delta Hep/\Delta Hep}$ $clap2^{-/-}$ mice compared with WT animals at 20 and 44 h post-infection by immunoblotting (Figures S1H and S1I). The abrogation of liver-stage infection in $clap1^{\Delta Hep/\Delta Hep}$ $clap2^{-/-}$ mice was accompanied by an elevation in serum liver transaminase (ALT) levels, peaking at 20 h post-infection, indicative of hepatocyte death or dysfunction, although ALT levels were comparatively low compared with that seen for systemic hepatitis (compare with Figure 6F, described below). This transaminitis was not observed in control animals (Figure 1F).

Our data indicated that infection of cIAP1/2-deficient mice with sporozoites was followed by an increase in TNF and TNFR1 levels and increased parasite clearance from the liver accompanied by mild transaminitis following infection compared with WT mice.

A Clinical-Stage IAP Antagonist Promotes Killing of *Plasmodium*-Infected Hepatocytes

We examined the therapeutic efficacy of targeting cIAPs using clinical-stage drugs. Birinapant has bivalency for its targets (cIAP1/2, XIAP) and causes a reduction in cIAP1 and cIAP2 levels through autoubiquitination and proteasomal degradation (Benetatos et al., 2014; Condon et al., 2014). We allometrically scaled the approximate clinical maximum tolerated dose (MTD) of birinapant (47 mg/m²) (Amaravadi et al., 2015) to treat mice with a single or two doses of drug following sporozoite infection. WT mice were intravenously (i.v.) injected with 1×10^4 sporozoites, and a single dose of birinapant was administered 18, 32, or 44 h post-infection. Alternatively, mice were treated with two doses of birinapant administered at 18 and 32 h post-infection or 18 and 44 h post-infection. All drug schedules reduced parasite liver burden, as determined by qPCR (Figure 2A). A single dose of birinapant administered 18 h post-infection was sufficient to delay and attenuate the blood stage parasitemia in infected animals compared with vehicle-treated controls (Figure 2B). This attenuation was followed by improved survival of birinapant-treated mice compared with controls (Figure 2C).

Our data using a large sporozoite inoculum suggested that IAP antagonists could help protect from infection by promoting TNF-induced death of infected hepatocytes. However, a physiological inoculum of typically tens to hundreds of sporozoites per mosquito bite (Frischknecht et al., 2004; Jin et al., 2007) might not generate sufficient TNF to synergize with IAP antagonists. To test a more physiological infectious challenge, mice were i.v. injected with 1,000 sporozoites, and a single dose of birinapant was administered 18 h post-infection. Importantly, we observed reductions in parasite liver load in animals treated with birinapant following infection compared with vehicle-treated controls (Figure 2D). To follow the development of liver infection, we used a GFP-luciferase-producing strain of *P. berghei* to image infected animals over time. We confirmed that birinapant reduced parasite biomass in the liver of infected mice and interfered with the establishment of patent infection compared with vehicle-treated mice following challenge with 1,000 sporozoites (Figures 2E and 2F; Figure S2).

Our data support the idea that birinapant promotes death of hepatocytes and the parasites within them, consequently causing a delay in the development of blood-stage malaria. However, an alternative hypothesis is that birinapant also affects
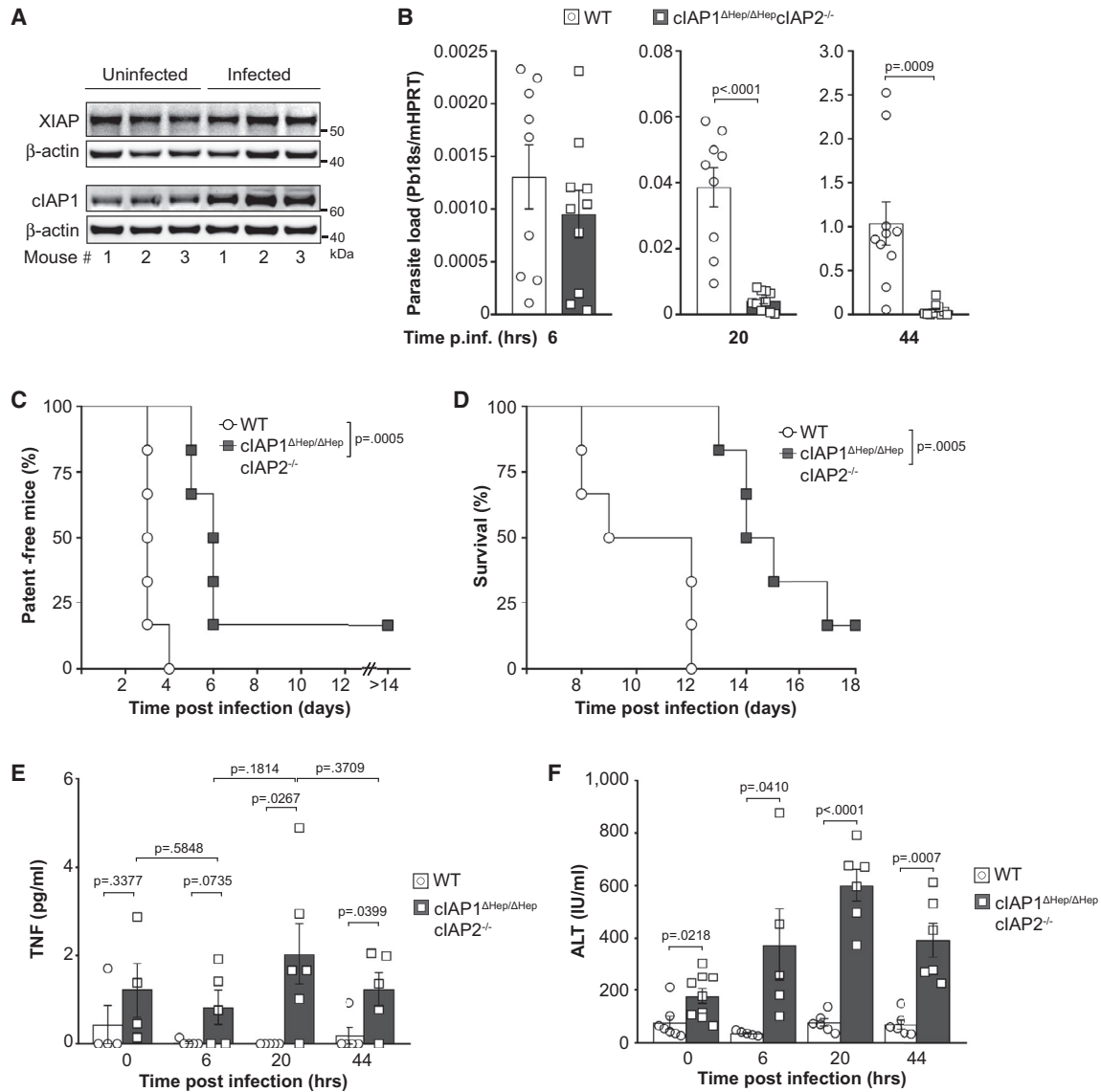
Figure 1. Genetic Loss of cIAP1/2 Promotes Clearance of *Plasmodium* Liver Stages

(A) Western blot analysis of XIAP and cIAP1 expression relative to β-actin in liver cell lysates from naive or infected (44 h later) mice across three biological replicates. See also Figures S1A and S1B for densitometry.

(B) Parasite liver load quantified using qPCR at the indicated time points following infection with 10,000 sporozoites (n = 9 or 10 per group).

(C) Time to first detection of patency following sporozoite infection. A single cIAP1/2-deficient animal did not develop blood-stage malaria at the completion of the experiment (14 days post-infection) (n = 6 per group).

(D) Kaplan-Meier plots showing time to ethical euthanasia in wild-type (WT) and gene-targeted animals. Mice were euthanized if there were any signs of cerebral malaria or if parasitemia was >15%.

(E) Serum TNF levels in infected mice (n = 4–6 per group). See also Figures S1C–S1G.

(F) Serum ALT (alanine aminotransferase) levels in infected mice (n = 5–9 mice per group).

Mean and SEM are shown (B, E, and F); each symbol represents an individual mouse (B–F). Data were pooled from two experiments (B). Data analysis was performed blinded to treatment groups.

asexual blood stages. To investigate this possibility, we transferred *P. berghei*-infected red blood cells (iRBCs) into naive WT mice and treated the animals with birinapant or vehicle at 18 h post-inoculation. The kinetics of parasitemia were comparable in birinapant- and vehicle-treated mice, indicating that

birinapant had no direct effect on parasitized red blood cells and circulating merozoites (Figure 2G).

To confirm the hypothesis that birinapant promotes death of hepatocytes, we investigated the presence of activated caspase-3, a cell death protease, in the livers of infected mice.

A

B

C

D

E

F

G

H

I
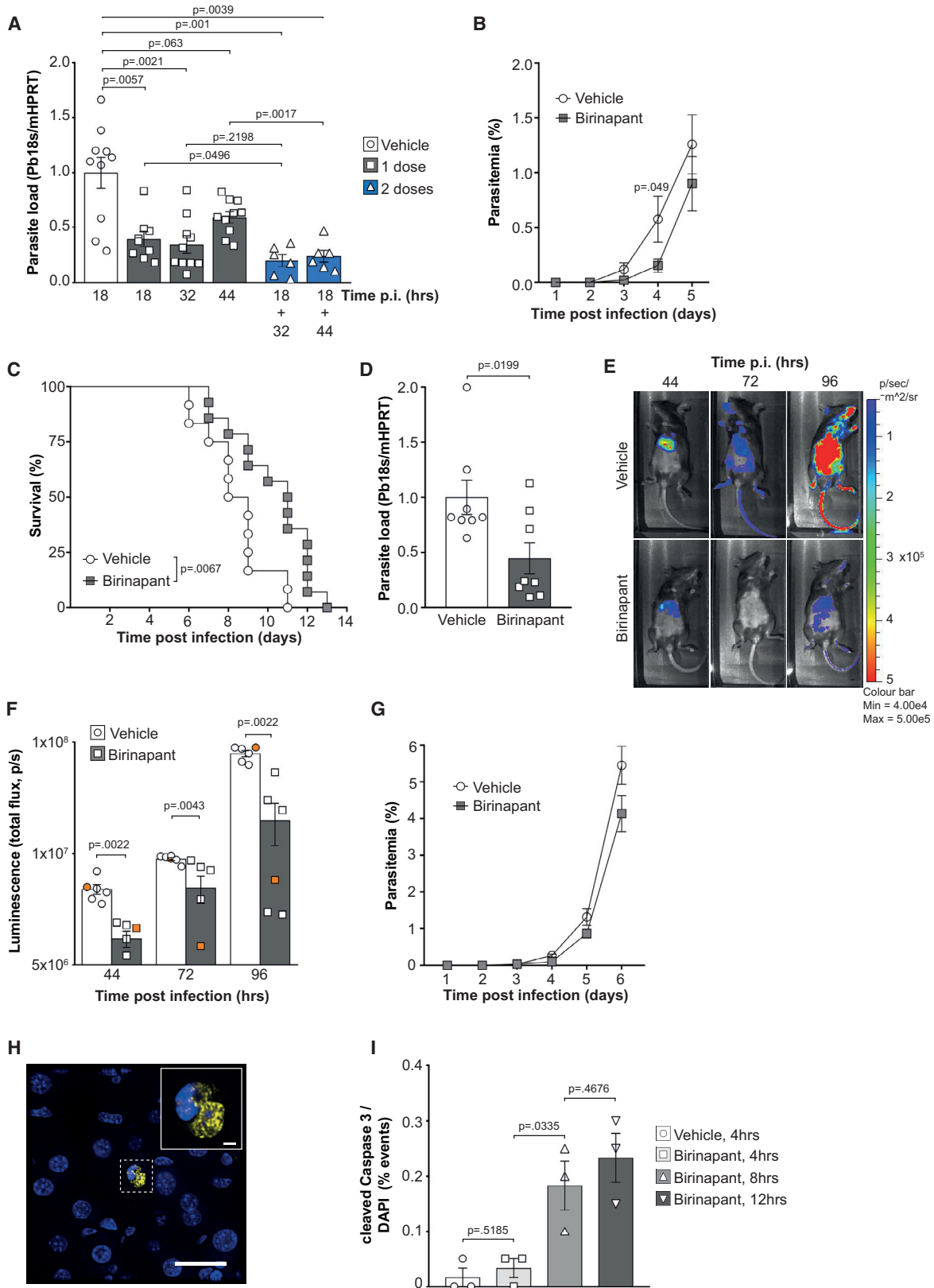
(legend on next page)

Immunofluorescence microscopy confirmed that hepatocyte death was occurring in the livers of infected mice at 4 and 8 h after birinapant treatment and that only a small number of total cells were dying (Figures 2H and 2I). These results demonstrate that an IAP antagonist promotes clearance of *Plasmodium* liver stages by inducing death of a small number of cells in the liver.

Birinapant Kills Liver Stages through TNF-Mediated Hepatocyte Apoptosis

To confirm our hypothesis that birinapant's efficacy was driven through death receptor signaling causing clearance of infected hepatocytes, we used gene-targeted mice that were deficient in the death ligands. Mice with a compound loss of TNF, TRAIL, and Fas ligand failed to respond to birinapant treatment and developed parasite liver loads that were comparable with those in vehicle-treated knockout animals and untreated littermate control mice (Figure 3A). This demonstrates that birinapant is not active against EEFs but is acting on host cells in a manner dependent upon one or more death ligands. To determine if one or all death ligands contributed to birinapant's efficacy, we next used transgenic mice that specifically lacked either Fas receptor in the liver (*Tnfsf6:Fas^{fl/fl}AlbCre*) or that were deficient only in TRAIL (*Tnfsf10:Trail^{-/-}*) or only in TNF (*Tnfsf2:Tnf^{-/-}*). Birinapant lost efficacy only in TNF-null animals (Figures 3B–3D), demonstrating that its efficacy is dependent on TNF.

TNF drives cell death predominantly through the induction of apoptosis, but under certain circumstances it can induce a lytic form of cell death called necroptosis. Caspase-8 is essential for the induction of apoptosis but not necroptosis. To confirm that birinapant was promoting TNF-mediated apoptosis, we infected mice that specifically lacked caspase-8 in hepatocytes (*Casp8^{fl/fl}AlbCre*). We found that birinapant had no efficacy in *Casp8^{fl/fl}AlbCre* mice (Figure 3E), indicating that the IAP antagonists promote clearance of *Plasmodium*-infected hepatocytes via TNF-driven apoptosis.

Hepatocyte death is accompanied by a transaminitis, and we found that a single dose of birinapant caused a greater degree of transaminitis in infected animals than in controls (Figure 3F). Birinapant treatment did not cause any major histological abnor-malities in uninfected or infected mice compared with vehicle controls, indicating that induction of apoptosis in mice was specifically associated with *P. berghei* infection (Figure S3). Birinapant treatment did not affect immune cell infiltrates in the liver of uninfected and infected mice compared with vehicle control (Figures S3B and S3C). However, the frequency of CD3$^+$ T cells (Figure S3B) and macrophages (Figure S3C) appeared greater in infected animals compared with uninfected mice regardless of treatment. Collectively the data showed that birinapant efficacy was mediated through the induction of TNF-driven apoptosis. Importantly, birinapant was neither killing parasites directly nor causing major hepatic destruction or collateral damage, indicating a degree of host cell selectivity consistent with the known low frequency of sporozoite-infected liver cells. In cancer clinical trials, IAP antagonists have not caused any major liver toxicity (Bai et al., 2014; Fulda, 2015).

Birinapant Promotes Liver Parasite Clearance following Infection by Mosquito Bites

Our findings that the IAP antagonist birinapant is efficacious against liver stages using a low sporozoite inoculum raised the possibility that IAP antagonists may be efficacious in the physiologically relevant setting of mosquito-driven transmission. We permitted *P. berghei*-infected mosquitoes to bite mice for 15 min, and animals were treated with one dose of birinapant 18 h post-exposure. We found that birinapant caused a significant reduction in parasite liver load compared with vehicle treatment (Figure 4A). This translated to a 1 day delay in detectable parasitemia, consistent with a >90% reduction in viable merozoites egressing the liver (Figure 4B). Thereafter, a substantial reduction in the level of parasitemia was observed at all time points in birinapant-treated animals compared with controls (Figure 4C). In keeping with the attenuation in parasitemia, we observed a significant improvement in disease progression and survival kinetics of birinapant-treated mice compared with vehicle controls (Figure 4D). These results indicate that birinapant promotes clearance of *P. berghei* liver infection and consequently blood-stage malaria infection in a natural transmission model.

Figure 2. Birinapant Promotes Clearance of Liver-Stage Parasites via Caspase-3-Positive Death of Hepatocytes

(A) Parasite liver load quantified using qPCR 52 h post-infection. Mice were i.v. infected with 10,000 sporozoites followed by one or two doses of birinapant or vehicle at the indicated time points (n = 6–10 per group).

(B) Mouse blood-stage parasitemia following 10,000-sporozoite challenge and a single birinapant or vehicle treatment at 18 h post-infection (n = 12–14 per group).

(C) Kaplan-Meier curves showing outcomes in mice following 10,000-sporozoite challenge and a single dose of birinapant or vehicle 18 h post-infection. Mice were euthanized if any signs of cerebral malaria were evident or if parasitemia reached >15% (n = 12–14 per group).

(D) Parasite liver load quantified using qPCR 44 h post-infection. Mice received a single dose of birinapant or vehicle at 18 h post-injection with 1,000 sporozoites (n = 8 per group).

(E) Representative IVIS imaging of mice from (F) (representative of n = 6 per group). All images of vehicle or birinapant treatment are the same animal over time. See also Figure S2 for all mice.

(F) Quantification of luminescence and parasite burden from (E) (n = 6 per group). Symbols in orange represent the animals shown in (E).

(G) Parasitemia measured by Giemsa smears following intraperitoneal infection of 10,000 *P. berghei*-infected red blood cells (iRBCs) and a single dose of birinapant or vehicle 18 h post-infection (n = 6 per group).

(H) Representative micrograph showing cleaved caspase-3 (yellow) and DAPI (blue) in the livers of mice following i.v. infection with 4×10^5 sporozoites followed by one dose of birinapant at 18 h post-infection and sample fixation 8 h thereafter. Scale bar: 20 μm.

(I) Quantification of cleaved caspase-3-positive events in relation to DAPI-positive events by immunofluorescence microscopy of liver sections (n = 3). Mice were infected and treated as above and livers fixed and analyzed at the indicated time points after treatment.

Mean and SEM are shown (A, B, D, F, and G). Data were pooled from two independent experiments (A–D, F, and G). Images in (E) are representative of ten independent experiments. Each symbol (A, D, and F) represents an individual mouse. Data analysis was performed blinded to treatment groups.
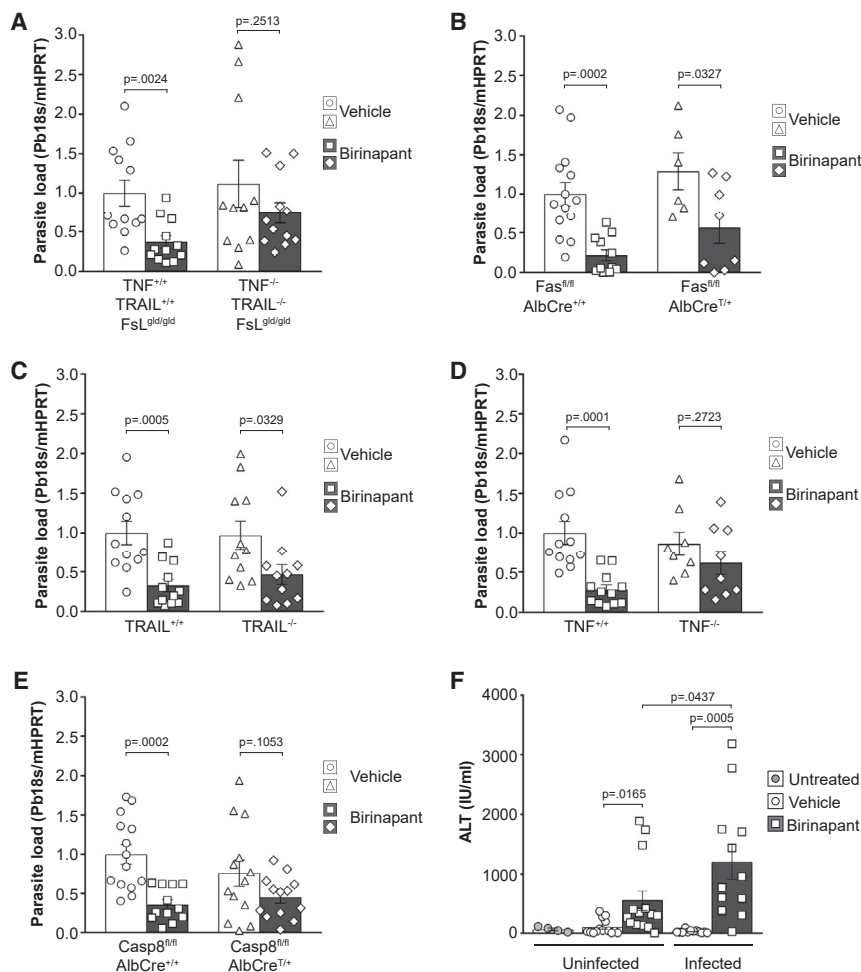
Figure 3. Birinapant's Efficacy in Killing Liver Stages Is Mediated through TNF-Induced Apoptosis of Host Cells

(A) RT-PCR quantification of liver parasites 44 h post-infection in control mice TNF TRAIL FasL triple mutant mice intravenously injected with 10,000 *P. berghei* sporozoites and treated with a single dose of birinapant or vehicle administered 18 h post-infection (n = 11 or 12 per group).

(B–E) As described in (A), RT-PCR quantification of liver parasites 44 hr post-infection in control mice and Fas receptor mutant (B), in control mice and TRAIL mutant mice (C), in control mice and TNF mutant mice (D), or in control mice and Caspase-8 mutant mice (E).

(F) Serum ALT levels quantified in uninfected or infected WT mice 16 h after the indicated treatments that where administered 18 h post-infection (n = 4–14 per group). See also Figure S3.

Data are shown as mean and SEM and were pooled from two independent experiments, and each symbol represents an individual mouse (A–F). Data analysis was performed blinded to treatment groups.

T cells have been shown to mediate immunity to liver-stage infection (Doolan et al., 2009; Kurup et al., 2019).

We found that birinapant-treated mice had more CD4$^+$, CD8$^+$, and activated CD44$^+$ T cells in the spleen, liver, and liver-draining lymph nodes after secondary infection compared with vehicle-treated mice and naive mice (which had never been infected) (Figure 5F; Figure S4). We also detected antibodies in the serum of birinapant-treated animals that were specific for sporozoites by immunofluorescence microscopy, but quantification of signal intensities suggested the antibodies generated may be in response to sporozoite challenge rather than as a result of birinapant treatment (Figure 5G; Figure S5). These data are consistent with birinapant, through the induction of apoptosis in infected cells, promoting acquisition of T cell-mediated immunity to re-infection.

An Orally Bioavailable Clinical Stage IAP Inhibitor Promotes Liver-Stage Death

We next determined if a chemically distinct IAP antagonist would be able to recapitulate the efficacy of birinapant in reducing parasite liver burden. The clinical-stage drug LCL-161 is a monovalent IAP antagonist that is orally bioavailable and has been assessed in multiple clinical trials, making this safe drug amenable to clinical translation (Houghton et al., 2012; Infante et al., 2014). We postulated that a drug that targets liver-stage infection would have to be administered as pre-emptive treatment because liver-stage infection is asymptomatic and transient. Therefore, we orally administered LCL-161 before infection (at −3 h), followed by once daily after sporozoite infection (at 18 and 40 h) (Figure 6A). We found that this LCL-161 regimen was highly

Birinapant Treatment during Primary Liver Infection Promotes Immunity to Sporozoite Re-challenge

Apoptosis of infected cells has been implicated in facilitating presentation of microbial antigens and promoting immunity (Campisi et al., 2014; Green et al., 2009). We investigated if birinapant-mediated apoptosis of *Plasmodium*-infected hepatocytes promotes immunity to re-challenge with sporozoites. Mice were first i.v. infected with 1,000 sporozoites and then treated with two doses of birinapant or vehicle at 18 and 32 h post-infection. This treatment regimen was selected because earlier experiments indicated that it caused the largest reduction in liver burden (Figure 5A). The efficacy of birinapant against the primary infection was confirmed using *in vivo* imaging (Figures 5A and 5B). All animals were then cured of any breakthrough parasitemia using chloroquine and pyrimethamine treatment. Four weeks after primary infection, mice were re-challenged with 1,000 sporozoites, and the kinetics of secondary infection were analyzed (Figures 5D and 5E). We found that mice treated with birinapant during primary infection had lower parasite liver burdens after re-challenge compared with vehicle treatment during the primary infection, indicating that birinapant induced enhanced immunity to secondary infection. Antibodies and

Figure 4. Birinapant Promotes Clearance of Liver Infection following Mosquito Transmission

(A) Parasite liver load quantified using RT-PCR 44 h post-infection. Mice were infected via exposure to ten mosquitoes and received a single dose of birinapant 18 h after mosquito exposure (n = 15 per group).

(B) Time to first detection of patency following infection via mosquito bites and a single birinapant or vehicle treatment at 18 h after mosquito exposure (n = 11 per group).

(C) Mouse parasitemia following infection via mosquito bites and a single birinapant or vehicle treatment at 18 h post-exposure (n = 11 per group).

(D) Kaplan-Meier curves showing outcomes in mice following infection by mosquito bites and a single birinapant or vehicle treatment 18 h after mosquito exposure. Mice were euthanized if there were any signs of cerebral malaria or if >15% of red blood cells were parasitized (n = 11 per group).

Mean and SEM are shown (A and C). Data were pooled from two independent experiments (A–D). Each symbol (A, B, and D) represents an individual mouse. Data analysis was performed blinded to treatment groups.

efficacious in causing sustained cIAP1 degradation in mice (Figure 6B) and reducing parasite liver burden compared with vehicle-treated animals, as measured by animal bioluminescent imaging (Figures 6C and 6D; Figure S6) and qPCR of livers from independent groups of mice (Figure 6E). Parasite clearance following LCL-161 administration was accompanied by a modest transaminitis (Figure 6F), consistent with hepatocyte death. The ALT levels detected were again low compared with control treatment with GalN + lipopolysaccharide (LPS), which induces systemic hepatitis (Kaufmann et al., 2009; Figure 6F). No histological abnormalities were present in the livers of infected and LCL-161-treated mice compared with vehicle controls, indicating that no large-scale off-target effects were occurring in the livers of IAP inhibitor-treated mice, in contrast to the systemic hepatitis model (Figure 6G). Hepatocyte death was again confirmed by the presence of cleaved caspase-3 in the livers of infected mice. Whereas LCL-161 caused very small numbers of caspase-3-positive cells, GalN + LPS caused a strong systemic effect (Figure 6H). This shows that an orally bioavailable IAP antagonist promotes clearance of *P. berghei* liver infection by acting on a small proportion of hepatocytes without systemic off-target effects. This suggests that different classes of IAP antagonists are likely to be efficacious, providing insights as to how such drugs might be clinically relevant as preventive therapy in malaria-endemic areas.

DISCUSSION

Strategies to eliminate malaria must integrate multiple factors, including vector and transmission control, targeting various stages of the parasite life cycle, and enhancing host immunity. Approaches must include elements that are refractory to the parasite's ability to develop resistance to directly acting antimalarials and its ability to evade immunity. In this study, we examined hepatocyte signaling pathways that permit or restrict progression of *Plasmodium* infection from liver to blood stage in an attempt to identify potential host molecular pathways that could be targeted to mitigate malaria disease progression.

We found that hepatocyte IAPs are important in maintaining host cell viability and the replicative niche that allows EEFs to develop into merozoites. We showed that IAPs could be targeted with the clinical-stage drugs birinapant and LCL-161 to promote clearance of liver infection in mice, which increased the pre-patent period. The death of liver-stage parasites occurred irrespective of sporozoite inoculum size and was additionally validated using a natural mode of transmission with mosquitoes. The major mediator of efficacy was through TNF-mediated apoptosis of hepatocytes that killed EEFs. This mechanism was sufficiently specific to prevent major liver damage. Indeed it has been shown that TNF inhibits the liver-stage growth of different *Plasmodium* species (Depinay et al., 2011; Nussler et al., 1991). Although IAP antagonists clearly induced apoptosis of hepatocytes, we cannot exclude that other changes in the liver environment could have contributed to killing parasites. However, because the target of birinapant and LCL-161 is IAPs located within the host cell, it would be difficult, if not impossible, for parasites to become resistant to treatment with IAP inhibitors. This supports host-targeted therapy as an attractive antimalarial avenue (Douglass et al., 2015; Kain et al., 2020; Kaushansky et al., 2013; Raphemot et al., 2019).

We used birinapant mostly as an IAP inhibitor in our experiments to define the mechanism of liver-stage clearance, primarily because of ease of administration in our animal models. Potential for translation to the human setting with *P. falciparum* or *P. vivax* remains a future goal but was partly validated using the IAP antagonist LCL-161, which is a monovalent, orally bioavailable drug. LCL-161 was at least equivalent to birinapant in its efficacy against *P. berghei* liver stages. Importantly, monovalent IAP antagonists are very well tolerated. Indeed,
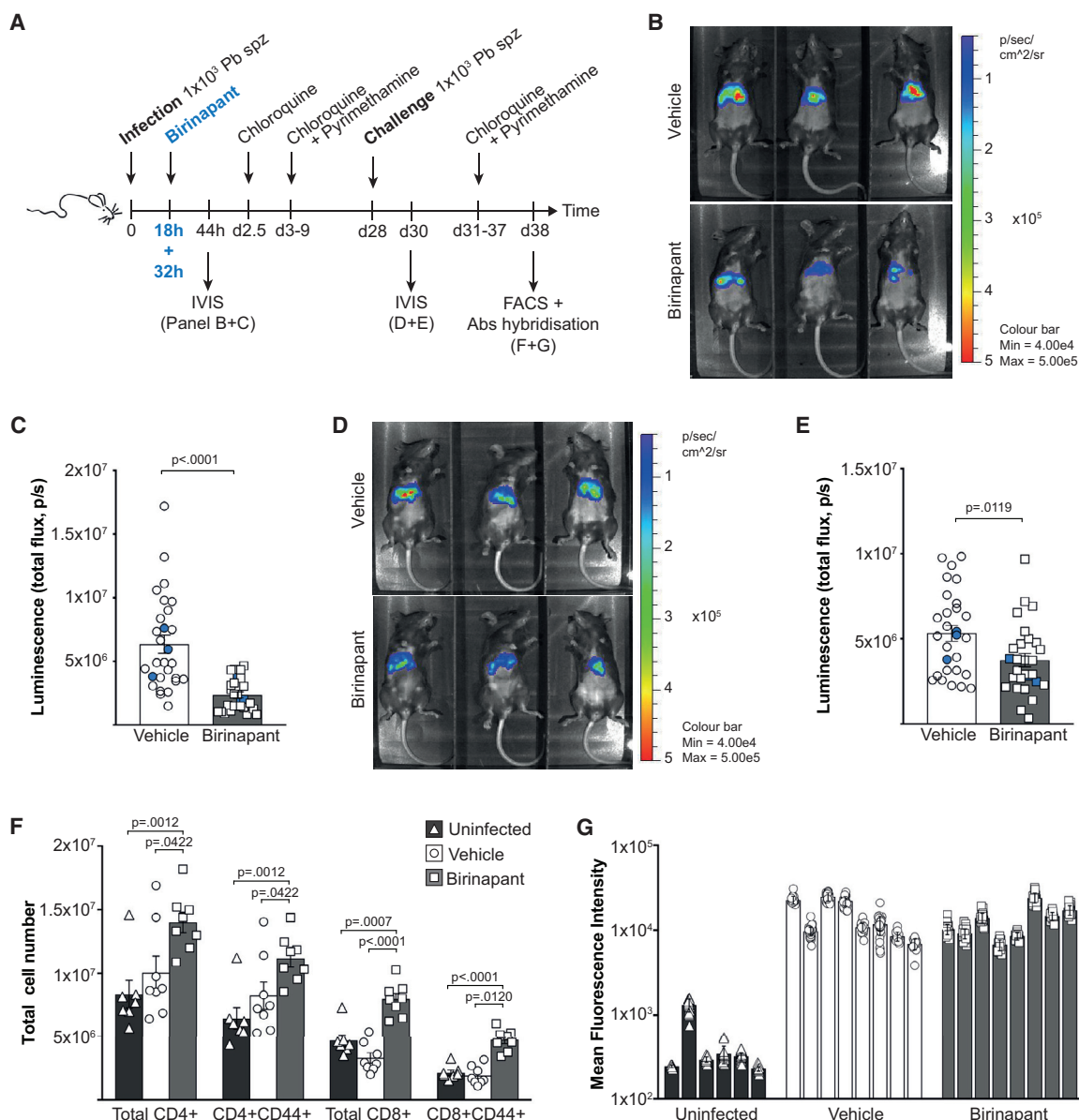
Figure 5. Birinapant-Mediated Apoptosis of Infected Liver Cells Promotes Protective Immunity Against Re-infection

(A) Schematic representation of experiments used to generate data in (B)–(G).

(B) Representative images generated using IVIS of infected mice (44 h) after two doses of birinapant or vehicle as shown in (A) (representative of n = 28 per group).

(C) Quantification of luminescence and parasite burden as shown in (B) (n = 28 per group). Symbols in blue represent the animals shown in (B).

(D) Representative images generated using IVIS of mice that were treated with birinapant and vehicle during primary infection, treated with antimalarials to prevent breakthrough infections, and challenged with sporozoites (representative of n = 28 per group). Images are from 44 h after the second infection.

(E) Quantification of luminescence and parasite burden as shown in (D) (n = 28 per group). Symbols in blue represent the animals shown in (D).

(F) Number and phenotypes of CD3^{+} T cells in mice shown in (D) and (E) (n = 8 per group). See also Figure S4.

(G) Quantification of fluorescence and sporozoite-specific antibody levels in mice shown in (D) and (E) (n = 8 per group). Uninfected mice indicate background levels. See also Figure S5.

Mean and SEM (C, E, and F) and mean and SD (G) are shown, and each symbol represents an individual mouse (C, E, and F). In (G), each column represents an individual mouse, each symbol a sporozoite. Data are pooled from two independent experiments (B–E). Data analysis was performed blinded to treatment groups.

extensive clinical testing has not revealed any dose-limiting toxicities, and an MTD was never defined for many of the monovalent IAP antagonists across numerous clinical trials (Bai et al., 2014; Derakhshan et al., 2017; Fulda, 2015). This extraordinary safety profile would allow daily dosing over extended periods that when combined with repeated exposure
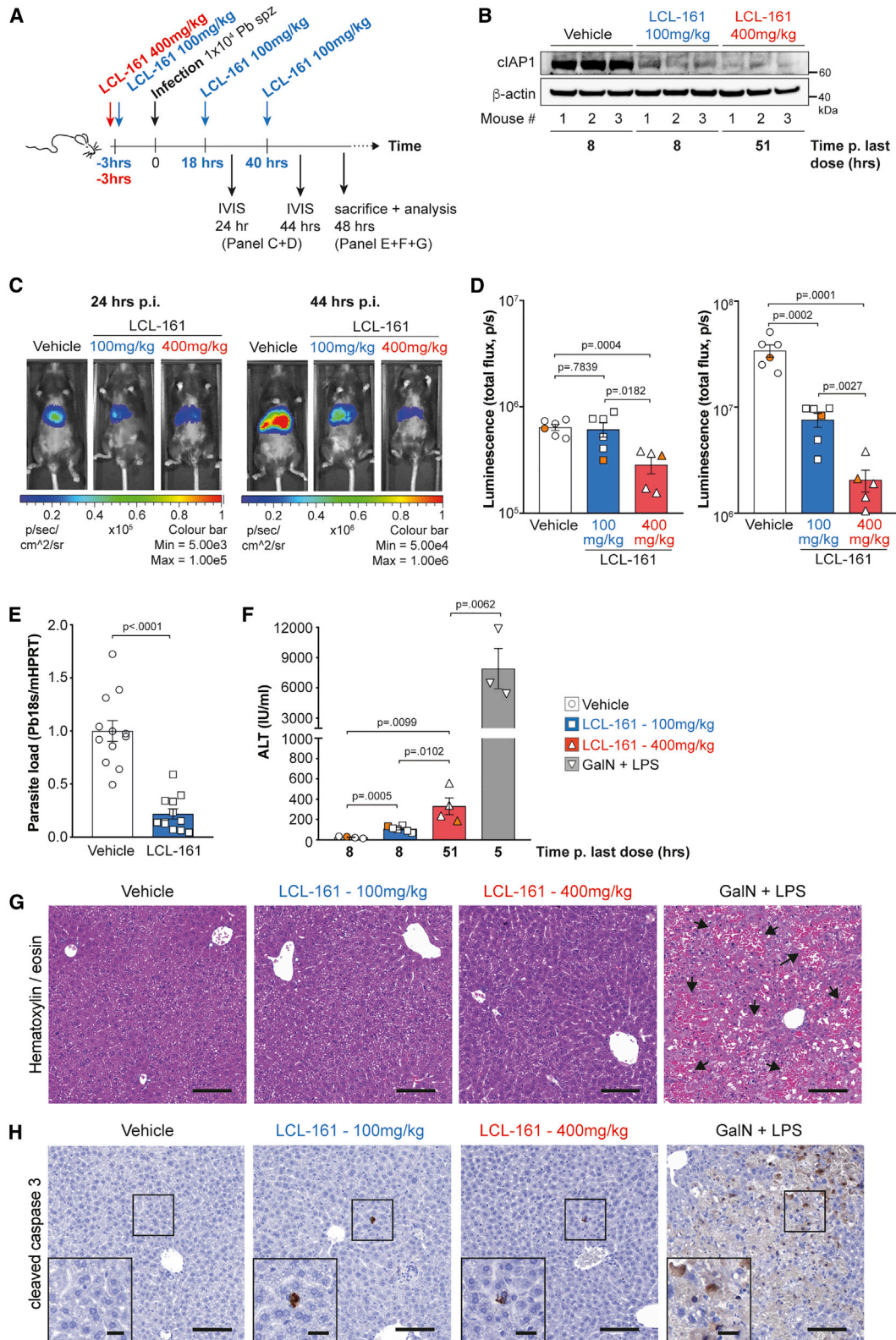
(legend on next page)

to malaria parasites (natural immunization) over a period coincident with administration of cIAP inhibitor treatment could induce protective immunity.

Our data showed that IAP antagonists induced TNF-mediated apoptosis that, in addition to clearing EEFs, promoted acquisition of immunity to pre-erythrocytic infection. This immunity was manifest as partial protection during liver infection following sporozoite re-challenge. Defining the precise mediators of this immunity was beyond the scope of the present study, but we provided evidence that T cell responses were produced. In endemic areas where re-infection is frequent, immunity enhancement via IAP inhibitors could be naturally boosted with re-exposure to malaria parasites and continued drug administration. This could eventually drive robust immunity to pre-erythrocytic stages and potentially blood stages if the arrested EEFs are sufficiently mature (Butler et al., 2011). The feasibility of such an approach is underscored by the tolerability and safety of some monovalent IAP antagonists that can be administered daily for protracted periods.

Our findings open up several areas of future investigation, including using IAP antagonists together with conventional antimalarials for prophylaxis in travelers visiting malaria-endemic areas. Such a strategy would mitigate the risk for drug resistance development. It will also be important to dissect how cIAPs are upregulated during infection and whether the parasite is actively driving this process by, for example, exporting effector proteins that modulate host cell responses. Most intriguing of all would be the potential use of IAP antagonists to clear dormant liver hypnozoites in people who have been exposed to P. vivax sporozoites. Despite successful treatment of P. vivax blood stages, EEFs can persist in the liver as hypnozoites (Adams and Mueller, 2017), and their reactivation leads to relapsing blood-stage malaria at any time, including years after initial exposure. Treatments for hypnozoites are limited to a few drugs that are associated with severe toxicities in people who lack the enzyme glucose-6-phosphate-dehydrogenase (Campo et al., 2015). Therefore, novel treatments for hypnozoites represent an enormous unmet need, and therapy that targets the host cell, as in this study, could be efficacious against them.

Our studies have offered several important insights regarding the biological role of IAPs in sustaining Plasmodium liver infection, their targetability for promoting clearance of infected hepatocytes, and the ability of IAP antagonists to promote pre-erythrocytic immunity. Such insights will form the basis of future studies with human malaria parasites and possibly clinical trials.

STAR★METHODS

Detailed methods are provided in the online version of this paper and include the following:

- KEY RESOURCES TABLE
- LEAD CONTACT AND MATERIALS AVAILABILITY
- EXPERIMENTAL MODEL AND SUBJECT DETAILS
  - Animal husbandry
  - Transgenic parasite line PbGFP-Luc$_{con}$
- METHOD DETAILS
  - In vivo cultivation of P. berghei sporozoites
  - Infection of mice with P. berghei sporozoites via intravenous tail vein injection
  - Infection of mice with P. berghei sporozoites by direct mosquito feeding
  - Infection of mice with iRBCs
  - Assessment of in vivo P. berghei liver infection by PCR
  - Assessment of in vivo P. berghei blood infection by blood smears
  - Quantification of in vivo P. berghei liver and blood infection by IVIS
  - IAP Antagonists
  - Alanine Aminotransferase Quantification
  - Systemic hepatitis model
  - Isolation of Hepatic and Splenic T cells
  - Cytokine Assays
  - Western Blotting
  - Immunofluorescence assay
  - Quantification and statistical analysis
  - Ethics Statement
- DATA AND CODE AVAILABILITY

SUPPLEMENTAL INFORMATION

Supplemental Information can be found online at https://doi.org/10.1016/j.celrep.2020.03.032.

Figure 6. The Clinical-Stage IAP Antagonist LCL-161 Promotes Elimination of Liver-Stage Parasites

(A) Schematic representation of experiments used to generate date in (B)–(H).

(B) Western blot analysis of cIAP1 expression relative to β-actin in liver cell lysates from infected WT mice after the indicated treatments at indicated time points after administration of last dose (see Figure 6A) across three biological replicates.

(C) Representative IVIS images of infected mice (24 h post-infection [p.i.], left; 44 h p.i., right) after indicated doses of LCL-161 or vehicle as shown in (A) (representative of n = 5 or 6 per group). All images of vehicle or LCL-161 treatment are the same animal at both time points. See also Figure S6.

(D) Quantification of luminescence and parasite burden as shown in (C) (n = 5 or 6 per group). Symbols in orange represent the animals shown in (C).

(E) Parasite liver load 44 h post-infection with 10,000 sporozoites and three once-daily oral doses of LCL-161 or vehicle quantified using qRT-PCR (n = 12 per group).

(F) Serum ALT levels quantified in infected WT mice after the indicated treatments and indicated time points after administration of last dose (n = 3–6 per group).

(G) Representative hematoxylin and eosin-stained liver sections after the indicated treatments 48 h post-infection. Black arrows indicate systemic liver damage. Scale bar: 100 μm.

(H) Representative liver sections after labeling for cleaved caspase-3 after the indicated treatments 48 h post-infection. Scale bar: 100 μm.

Mean and SEM (D–F) are shown, and each symbol represents an individual mouse (D–F). Data are pooled from two independent experiments (E). Data analysis was performed blinded to treatment groups.

AUTHOR CONTRIBUTIONS

G.E., M.P., and J.A.B. conceived the project, designed experiments, analyzed and interpreted data, and prepared the manuscript. G.E., S.L., M.T.O., R.W.J.S., M.D., P.R., A.S.P.Y., S.E., L.I., P.A., L.M., C.A., and J.S. performed experiments or generated reagents and analyzed data. All authors assisted with writing the manuscript.

DECLARATION OF INTERESTS

The authors declare no competing interests.

REFERENCES

Adams, J.H., and Mueller, I. (2017). The biology of Plasmodium vivax. Cold Spring Harb. Perspect. Med. 7, a025585.

Albuquerque, S.S., Carret, C., Grosso, A.R., Tarun, A.S., Peng, X., Kappe, S.H.I., Prudêncio, M., and Mota, M.M. (2009). Host cell transcriptional profiling during malaria liver stage infection reveals a coordinated and sequential set of biological events. BMC Genomics 10, 270.

Amaravadi, R.K., Schilder, R.J., Martin, L.P., Levin, M., Graham, M.A., Weng, D.E., and Adjei, A.A. (2015). A phase I study of the SMAC-Mimetic birinapant in adults with refractory solid tumors or lymphoma. Mol. Cancer Ther. 14, 2569–2575.

Armistead, J.S., Jennison, C., O'Neill, M.T., Lopaticki, S., Liehl, P., Hanson, K.K., Annoura, T., Rajasekaran, P., Erickson, S.M., Tonkin, C.J., et al. (2018). Plasmodium falciparum subtilisin-like ookinete protein SOPT plays an important and conserved role during ookinete infection of the Anopheles stephensi midgut. Mol. Microbiol. 109, 458–473.

Ashkenazi, A., and Dixit, V.M. (1998). Death receptors: signaling and modulation. Science 281, 1305–1308.

Bai, L., Smith, D.C., and Wang, S. (2014). Small-molecule SMAC mimetics as new cancer therapeutics. Pharmacol. Ther. 144, 82–95.

Benetatos, C.A., Mitsuuchi, Y., Burns, J.M., Neiman, E.M., Condon, S.M., Yu, G., Seipel, M.E., Kapoor, G.S., Laporte, M.G., Rippin, S.R., et al. (2014). Birinapant (TL32711), a bivalent SMAC mimetic, targets TRAF2-associated cIAPs, abrogates TNF-induced NF-κB activation, and is active in patient-derived xenograft models. Mol. Cancer Ther. 13, 867–879.

Bertrand, M.J.M., Milutinovic, S., Dickson, K.M., Ho, W.C., Boudreault, A., Durkin, J., Gillard, J.W., Jaquith, J.B., Morris, S.J., and Barker, P.A. (2008). cIAP1 and cIAP2 facilitate cancer cell survival by functioning as E3 ligases that promote RIP1 ubiquitination. Mol. Cell 30, 689–700.

Butler, N.S., Schmidt, N.W., Vaughan, A.M., Aly, A.S., Kappe, S.H.I., and Harty, J.T. (2011). Superior antimalarial immunity after vaccination with late liver stage-arresting genetically attenuated parasites. Cell Host Microbe 9, 451–462.

Campisi, L., Cummings, R.J., and Blander, J.M. (2014). Death-defining immune responses after apoptosis. Am. J. Transplant. 14, 1488–1498.

Campo, B., Vandal, O., Wesche, D.L., and Burrows, J.N. (2015). Killing the hypnozoite—drug discovery approaches to prevent relapse in Plasmodium vivax. Pathog. Glob. Health 109, 107–122.

Condon, S.M., Mitsuuchi, Y., Deng, Y., LaPorte, M.G., Rippin, S.R., Haimowitz, T., Alexander, M.D., Kumar, P.T., Hendi, M.S., Lee, Y.-H., et al. (2014). Birinapant, a smac-mimetic with improved tolerability for the treatment of solid tumors and hematological malignancies. J. Med. Chem. 57, 3666–3677.

Depinay, N., Franetich, J.F., Grüner, A.C., Mauduit, M., Chavatte, J.-M., Luty, A.J.F., van Gemert, G.J., Sauerwein, R.W., Siksik, J.-M., Hannoun, L., et al. (2011). Inhibitory effect of TNF-α on malaria pre-erythrocytic stage development: influence of host hepatocyte/parasite combinations. PLoS ONE 6, e17464.

Derakhshan, A., Chen, Z., and Van Waes, C. (2017). Therapeutic small molecules target inhibitor of apoptosis proteins in cancers with deregulation of extrinsic and intrinsic cell death pathways. Clin. Cancer Res. 23, 1379–1387.

Doolan, D.L., Dobaño, C., and Baird, J.K. (2009). Acquired immunity to malaria. Clin. Microbiol. Rev. 22, 13–36.

Douglass, A.N., Kain, H.S., Abdullahi, M., Arang, N., Austin, L.S., Mikolajczak, S.A., Billman, Z.P., Hume, J.C.C., Murphy, S.C., Kappe, S.H.I., and Kaushansky, A. (2015). Host-based prophylaxis successfully targets liver stage malaria parasites. Mol. Ther. 23, 857–865.

Ebert, G., Allison, C., Preston, S., Cooney, J., Toe, J.G., Stutz, M.D., Ojaimi, S., Baschuk, N., Nachbur, U., Torresi, J., et al. (2015a). Eliminating hepatitis B by antagonizing cellular inhibitors of apoptosis. Proc. Natl. Acad. Sci. U S A 112, 5803–5808.

Ebert, G., Preston, S., Allison, C., Cooney, J., Toe, J.G., Stutz, M.D., Ojaimi, S., Scott, H.W., Baschuk, N., Nachbur, U., et al. (2015b). Cellular inhibitor of apoptosis proteins prevent clearance of hepatitis B virus. Proc. Natl. Acad. Sci. U S A 112, 5797–5802.

Frischknecht, F., Baldacci, P., Martin, B., Zimmer, C., Thiberge, S., Olivo-Marin, J.-C., Shorte, S.L., and Ménard, R. (2004). Imaging movement of malaria parasites during transmission by Anopheles mosquitoes. Cell. Microbiol. 6, 687–694.

Fulda, S. (2015). Promises and challenges of Smac mimetics as cancer therapeutics. Clin. Cancer Res. 21, 5030–5036.

Green, D.R., Ferguson, T., Zitvogel, L., and Kroemer, G. (2009). Immunogenic and tolerogenic cell death. Nat. Rev. Immunol. 9, 353–363.

Houghton, P.J., Kang, M.H., Reynolds, C.P., Morton, C.L., Kolb, E.A., Gorlick, R., Keir, S.T., Carol, H., Lock, R., Maris, J.M., et al. (2012). Initial testing (stage 1) of LCL161, a SMAC mimetic, by the Pediatric Preclinical Testing Program. Pediatr. Blood Cancer 58, 636–639.

Infante, J.R., Dees, E.C., Olszanski, A.J., Dhuria, S.V., Sen, S., Cameron, S., and Cohen, R.B. (2014). Phase I dose-escalation study of LCL161, an oral inhibitor of apoptosis proteins inhibitor, in patients with advanced solid tumors. J. Clin. Oncol. 32, 3103–3110.

Item, F., Wueest, S., Lemos, V., Stein, S., Lucchini, F.C., Denzler, R., Fisser, M.C., Challa, T.D., Pirinen, E., Kim, Y., et al. (2017). Fas cell surface death receptor controls hepatic lipid metabolism by regulating mitochondrial function. Nat. Commun. 8, 480.

Janse, C.J., Franke-Fayard, B., Mair, G.R., Ramesar, J., Thiel, C., Engelmann, S., Matuschewski, K., van Gemert, G.J., Sauerwein, R.W., and Waters, A.P. (2006). High efficiency transfection of Plasmodium berghei facilitates novel selection procedures. Mol. Biochem. Parasitol. 145, 60–70.

Jin, Y., Kebaier, C., and Vanderberg, J. (2007). Direct microscopic quantification of dynamics of Plasmodium berghei sporozoite transmission from mosquitoes to mice. Infect. Immun. 75, 5532–5539.

Kain, H.S., Glennon, E.K.K., Vijayan, K., Arang, N., Douglass, A.N., Fortin, C.L., Zuck, M., Lewis, A.J., Whiteside, S.L., Dudgeon, D.R., et al. (2020). Liver stage malaria infection is controlled by host regulators of lipid peroxidation. Cell Death Differ. 27, 44–54.

Kaufmann, T., Jost, P.J., Pellegrini, M., Puthalakath, H., Gugasyan, R., Gerondakis, S., Cretney, E., Smyth, M.J., Silke, J., Hakem, R., et al. (2009). Fatal hepatitis mediated by tumor necrosis factor TNFalpha requires caspase-8 and involves the BH3-only proteins Bid and Bim. Immunity 30, 56–66.

Kaushansky, A., Metzger, P.G., Douglass, A.N., Mikolajczak, S.A., Lakshmanan, V., Kain, H.S., and Kappe, S.H. (2013). Malaria parasite liver stages

render host hepatocytes susceptible to mitochondria-initiated apoptosis. Cell Death Dis. 4, e762.

Kurup, S.P., Butler, N.S., and Harty, J.T. (2019). T cell-mediated immunity to malaria. Nat. Rev. Immunol. 19, 457–471.

Lalaoui, N., and Vaux, D.L. (2018). Recent advances in understanding inhibitor of apoptosis proteins. F1000Res. 7, 1889.

Lamkanfi, M., and Dixit, V.M. (2010). Manipulation of host cell death pathways during microbial infections. Cell Host Microbe 8, 44–54.

Leirião, P., Albuquerque, S.S., Corso, S., van Gemert, G.J., Sauerwein, R.W., Rodriguez, A., Giordano, S., and Mota, M.M. (2005). HGF/MET signalling protects Plasmodium-infected host cells from apoptosis. Cell. Microbiol. 7, 603–609.

Liehl, P., Zuzarte-Luís, V., Chan, J., Zillinger, T., Baptista, F., Carapau, D., Konert, M., Hanson, K.K., Carret, C., Lassnig, C., et al. (2014). Host-cell sensors for Plasmodium activate innate immunity against liver-stage infection. Nat. Med. 20, 47–53.

Mahoney, D.J., Cheung, H.H., Mrad, R.L., Plenchette, S., Simard, C., Enwere, E., Arora, V., Mak, T.W., Lacasse, E.C., Waring, J., and Korneluk, R.G. (2008). Both cIAP1 and cIAP2 regulate TNFalpha-mediated NF-kappaB activation. Proc. Natl. Acad. Sci. U S A 105, 11778–11783.

Micheau, O., and Tschopp, J. (2003). Induction of TNF receptor I-mediated apoptosis via two sequential signaling complexes. Cell 114, 181–190.

Nussler, A., Pied, S., Goma, J., Rénia, L., Miltgen, F., Grau, G.E., and Mazier, D. (1991). TNF inhibits malaria hepatic stages in vitro via synthesis of IL-6. Int. Immunol. 3, 317–321.

Pasparakis, M., Alexopoulou, L., Episkopou, V., and Kollias, G. (1996). Immune and inflammatory responses in TNF alpha-deficient mice: a critical requirement for TNF alpha in the formation of primary B cell follicles, follicular dendritic cell networks and germinal centers, and in the maturation of the humoral immune response. J. Exp. Med. 184, 1397–1411.

Raphemot, R., Toro-Moreno, M., Lu, K.-Y., Posfai, D., and Derbyshire, E.R. (2019). Discovery of druggable host factors critical to plasmodium liver-stage infection. Cell Chem. Biol. 26, 1253–1262.e5.

Sedger, L.M., Glaccum, M.B., Schuh, J.C.L., Kanaly, S.T., Williamson, E., Kayagaki, N., Yun, T., Smolak, P., Le, T., Goodwin, R., and Gliniak, B. (2002). Characterization of the in vivo function of TNF-alpha-related apoptosis-inducing ligand, TRAIL/Apo2L, using TRAIL/Apo2L gene-deficient mice. Eur. J. Immunol. 32, 2246–2254.

Taylor, S.M., and Fairhurst, R.M. (2014). Malaria parasites and red cell variants: when a house is not a home. Curr. Opin. Hematol. 21, 193–200.

van de Sand, C., Horstmann, S., Schmidt, A., Sturm, A., Bolte, S., Krueger, A., Lütgehetmann, M., Pollok, J.-M., Libert, C., and Heussler, V.T. (2005). The liver stage of Plasmodium berghei inhibits host cell apoptosis. Mol. Microbiol. 58, 731–742.

Varfolomeev, E., Blankenship, J.W., Wayson, S.M., Fedorova, A.V., Kayagaki, N., Garg, P., Zobel, K., Dynek, J.N., Elliott, L.O., Wallweber, H.J.A., et al. (2007). IAP antagonists induce autoubiquitination of c-IAPs, NF-kappaB activation, and TNFalpha-dependent apoptosis. Cell 131, 669–681.

Varfolomeev, E., Goncharov, T., Fedorova, A.V., Dynek, J.N., Zobel, K., Deshayes, K., Fairbrother, W.J., and Vucic, D. (2008). c-IAP1 and c-IAP2 are critical mediators of tumor necrosis factor alpha (TNFalpha)-induced NF-kappaB activation. J. Biol. Chem. 283, 24295–24299.

Vaughan, A.M., and Kappe, S.H.I. (2017). Malaria parasite liver infection and exoerythrocytic biology. Cold Spring Harb. Perspect. Med. 7, a025486.

Vince, J.E., Wong, W.W.-L., Khan, N., Feltham, R., Chau, D., Ahmed, A.U., Benetatos, C.A., Chunduru, S.K., Condon, S.M., McKinlay, M., et al. (2007). IAP antagonists target cIAP1 to induce TNFalpha-dependent apoptosis. Cell 131, 682–693.

Weiss, D.J., Lucas, T.C.D., Nguyen, M., Nandi, A.K., Bisanzio, D., Battle, K.E., Cameron, E., Twohig, K.A., Pfeffer, D.A., Rozier, J.A., et al. (2019). Mapping the global prevalence, incidence, and mortality of Plasmodium falciparum, 2000-17: a spatial and temporal modelling study. Lancet 394, 322–331.

Yatim, N., and Albert, M.L. (2011). Dying to replicate: the orchestration of the viral life cycle, cell death pathways, and immunity. Immunity 35, 478–490.

Zitvogel, L., Kepp, O., and Kroemer, G. (2010). Decoding cell death signals in inflammation and immunity. Cell 140, 798–804.

STAR★METHODS

KEY RESOURCES TABLE

REAGENT or RESOURCE	SOURCE	IDENTIFIER
Antibodies		
cIAP1; rabbit; 1:1000	In house antibody	N/A
TNFR1; hamster; 1:1,000; mab430	R&D Systems	MAB430-100
β-actin HRP; rabbit; 1:3,000	Cell Signaling Technology	5125S
CD3 IHC	Dako	Cat#A0452
F4/80 IHC	In house	N/A
CD3; PerCP; clone 1452C11	BD Biosciences	553067
CD4; Pacific Blue; clone GK1.5	BD Biosciences	558107
CD8; PE; clone 53–6.7	BD Biosciences	553032
CD44; FITC; clone IM7	BD Biosciences	561859
Cleaved caspase 3; IF and IHC; rabbit; 1:300	Cell Signaling Technology	9661
Goat anti-mouse-A594	Abcam	ab150116
Goat anti-Rabbit IgG HRP	Dako	P0448
Goat ant-rabbit biotin; IHC; 1:300	Vector Laboratories	PK-8800
Goat anti-rabbit Opal™570; cleaved caspase3 IF; 1:500	Perkin Elmer	FP1488001KT
Critical Commercial Assays		
Cytometric Bead Array (CBA) Flex System Kit	BD Bioscience	TNF: 558299
CBA Flex System Kit	BD Bioscience	IL-6: 558301
CBA Flex System Kit	BD Bioscience	IL-1β: 560232
CBA Flex System Kit	BD Bioscience	IL-17A: 560283
CBA Flex System Kit	BD Bioscience	IL-12p70: 560151
CBA Flex System Kit	BD Bioscience	GM-CSF: 558347
Mouse/Rat Soluble Protein Master Buffer Kit	BD Bioscience	558267
SensiFast cDNA synthesis kit	Bioline	BIO-65053
Pan T Cell Isolation Kit II, mouse	Miltenyi Biotech	130-095-130
Vectastain ABC Kit (HRP)	Vector Laboratories	PK-8800
Experimental Models: Organisms/Strains		
Mouse: C57BL/6 WT	In house	N/A
Mouse: C57BL/6 – cIAP1$^{\Delta Hep/\Delta Hep}$cIAP2$^{-/-}$	In house	(Ebert et al., 2015b)
Mouse: C57BL/6 - TNF$^{-/-}$TRAIL$^{-/-}$FasL$^{-gld/gld}$	This study	N/A
Mouse: C57BL/6 - Fas$^{fl/fl}$AlbCre	In house	(Item et al., 2017)
Mouse: C57BL/6 - TRAIL$^{-/-}$	In house	(Sedger et al., 2002)
Mouse: C57BL/6 - TNF$^{-/-}$	In house	(Pasparakis et al., 1996)
Mouse: C57BL/6 – Casp8$^{fl/fl}$AlbCre	In house	(Kaufmann et al., 2009)
Plasmodium: *P. berghei* ANKA with gfp::luc@eef1a. Line 676, m1 clone 1	Leiden University Medical Centre	676m1cl1 (RMgm-29)
Oligonucleotides		
Pb18S fw	IDT	(Liehl et al., 2014)
Pb18S rev	IDT	(Liehl et al., 2014)
mHPRT fw	IDT	(Liehl et al., 2014)
mHPRT rev	IDT	(Liehl et al., 2014)
Reagents		
TRI Reagent	Sigma	T9424
Ethidium bromide	BioRad	1610433

(*Continued on next page*)

Continued

REAGENT or RESOURCE	SOURCE	IDENTIFIER
D-Luciferin - K+ Salt Bioluminescent Substrate	PerkinElmer	122799
Triton X-100	Sigma-Aldrich	T8787
Glycerol	Ajax Finechem	AJA242
Percoll PLUS	Sigma-Aldrich	E0414
Birinapant	TetraLogic/Medivir	N/A
LCL-161	Novartis	N/A
D-(+)-Galactosamine hydrochloride	Sigma-Aldrich	G0500
Lipopolysaccharide from E.coli	Sigma-Aldrich	L2880
Software and Algorithms		
FIJI software	ImageJ	N/A
FlowJo Software	FlowJo LLC	N/A
Prism 7	GraphPad	N/A
Other		
LightCycler 480 Instrument II	Roche	05015243001
Transaminase assay	Roche	Cobas e411
TissueLyser II	QIAGEN	85300
IVIS Spectrum, Xenogen	PerkinElmer	124262

LEAD CONTACT AND MATERIALS AVAILABILITY

Reagents generated in this study are available from the Lead Contact, Justin A. Boddey (boddey@wehi.edu.au), with a completed Materials Transfer Agreement.

EXPERIMENTAL MODEL AND SUBJECT DETAILS

Animal husbandry
The Walter and Eliza Hall Institute of Medical Research Animal Ethics Committee reviewed and approved all animal experiments (AEC Project 2016.008). Six to 9 week old C57BL/6 mice of both genders were used in experiments. Gene targeted C57BL/6 animals, except $Tnf^{-/-}Trail^{-/-}FasL^{gld/gld}$, have been characterized previously: $clap1^{\Delta Hep/\Delta Hep}$ $clap2^{-/-}$ (Ebert et al., 2015b); $Tnf^{-/-}$ (Pasparakis et al., 1996); $Trail^{-/-}$ (Sedger et al., 2002); $Fas^{fl/fl}AlbCre$ (Item et al., 2017) and $Casp8^{fl/fl}AlbCre$ (Kaufmann et al., 2009). *P. berghei* infected mice were euthanized if animals showed any signs of cerebral malaria or if > 15% of red blood cells were parasitized.

Transgenic parasite line PbGFP-Luc_con
*Pb*GFP-Luc_CON contains the *gfp-luc* fusion gene under control of the constitutive *eef1α* promoter, integrated into the silent *230p* gene locus (PBANKA_030600); the line does not contain a drug-selectable marker (Janse et al., 2006).

METHOD DETAILS

In vivo cultivation of P. berghei sporozoites
To produce *P. berghei* sporozoites for infection, Swiss Webster 'donor' mice were infected via the intraperitoneal (i.p.) route with blood stage *P. berghei* ANKA *Pb*GFP-Luc_con parasites. Parasitaemia was monitored by Giemsa-stained tail blood smears. Four days post i.p. injection, red blood cells from these infected donor mice were transferred to naive mice via i.p. injection, which were used for direct feeding assays (DFAs) at four days post-inoculation. Mice with ≥ 1% parasitaemia and exhibiting exflagellation of microgametes by microscopy at 40x magnification were, anesthetized with ketamine/xylazine via i.p. inoculation, and individually placed on top of a single container of 50 female *An. stephensi* (3–5 days old) mosquitoes. Mosquitoes were allowed to feed on mice for 15 min, after which any unfed mosquitoes were collected and discarded. Numbers of midgut oocysts and salivary gland sporozoites per mosquito were determined at 14 days and 21 days post-blood feeding, respectively, as described above. At 21 days post-blood feeding, salivary glands were dissected from cold-anesthetized and ethanol killed mosquitoes. Salivary glands were pelleted at 3000 *g* for 3 minutes at 4°C. The salivary gland pellet was crushed with a plastic pestle (Scienceware 19923-0000), in a 1.5ml tube, recentrifuged for 1 minute at 3000 *g* and crushed a second time. A 500 μL tube with 26 gauge needle hole in the bottom was lightly packed with ∼200 μL of glass wool (Supelco, silane treated 2-0411), and placed inside a standard 1.5 mL Eppendorf tube. Crushed salivary glands were passed through the glasswool filter in 150 μL aliquots and centrifuged for 120 s at 1200 *g* and sporozoite filtrate

collected in a 1.5 mL tube on ice. 10 μL of sporozoite suspension, either pure or diluted by as much as 1:20, was placed onto a hae-mocytometer counting chamber (Assistent, Neubauer improved) and allowed to settle for 8 minutes in a humidity chamber prior to counting under phase at 400x magnification (Armistead et al., 2018).

Infection of mice with P. berghei sporozoites via intravenous tail vein injection

Mice were anesthetized with ketamine/xylazine via i.p. inoculation, and individually placed on top of a single container of 10 female *A. stephensi* mosquitoes, 21 days post-blood feeding respectively, as described above. Mosquitoes were allowed to feed on mice for 15 min and fed mosquitoes were collected and ethanol-killed afterward. Mosquitoes were dissected for salivary glands and assessed for sporozoite positivity as described above.

Infection of mice with P. berghei sporozoites by direct mosquito feeding

Mice were anesthetized with ketamine/xylazine via i.p. injection, and individually placed on top of a single container of 10 female *A. stephensi* mosquitoes that were aged to 21 days post initial feeding, as described above. Mosquitoes were allowed to feed on mice for 15 min and fed mosquitoes were collected and ethanol-killed afterward. Infection of mosquitoes was confirmed by dissec-tion of salivary glands and determination of sporozoite positivity through, as described above.

Infection of mice with iRBCs

To measure the effect of birinapant on asexual blood stage growth, mice were infected by intraperitoneal injected of 10,000 *P. berghei* ANKA iRBCs taken from a donor mouse. Mice were injected intraperitoneally with 30 mg/kg birinapant 18 hours post infec-tion with iRBCs and parasitemia was monitored daily by performing light microscopy of Giemsa-staining tail blood smears.

Assessment of *in vivo* P. berghei liver infection by PCR

At 44 hr post-infection, whole livers were dissected, and single cell suspensions generated with cell strainers. RNA was purified using TRI Reagent (Sigma) and cDNA prepared using a SensiFast cDNA synthesis kit (Bioline) according to manufacturers' instructions. Quantitative RT-PCR was performed using a LightCycler 480 (Roche) to measure crossing points for the *P. berghei* 18S ribosomal RNA subunit and mouse hypoxanthine guanine phosphoribosyl transferase (Hprt) housekeeping gene using ΔC_T and oligonucleo-tides listed in Key Resources Table (Liehl et al., 2014). Gene expression was calculated using the $\Delta\Delta C_T$ method, with the mean of the control group as calibrator to which other samples were compared.

Assessment of *in vivo* P. berghei blood infection by blood smears

To assess blood-stage infection, parasitaemia was monitored daily by examination of Giemsa-stained thin blood smears. Animals were observed daily for signs of severe disease and those that developed hyperparasitaemia (> 15%), anemia, or neurological symp-toms were CO_2 euthanized.

Quantification of *in vivo* P. berghei liver and blood infection by IVIS

To non-invasively monitor liver and blood stage infection at the indicates time points, mice were intraperitoneally (i.p.) injected with 200 μL of XenoLight D-Luciferin - K+ Salt Bioluminescent Substrate (PerkinElmer, Waltham, MA) and general anesthesia was induced by isoflurane inhalation (2% isoflurane in oxygen). Animals were imaged within 10 minutes of luciferin injection using the IVIS Spec-trum (Xenogen, PerkinElmer). To image 3 animals at a time, the instrument was set up with a 21.6 cm field of view, medium binning factor and an exposure time of 180 s.

IAP Antagonists

Birinapant was dissolved in DMSO and injected intraperitoneally at indicated time points at a concentration of 30 mg/kg. LCL-161 was dissolved in 30% (vol/vol) 0.1 M HCl, 70% (vol/vol) 0.1 M NaOAc (pH 4.63) and 3 doses at a concentration of 100 mg/kg were administered orally at indicated time points.

Alanine Aminotransferase Quantification

Serum levels of alanine aminotranferase (ALT) were measured using the activated alanine aminotransferase assay on an Architect c4000 analyzer (Abbott).

Systemic hepatitis model

Mice were injected i.p. with 100 ng LPS (Sigma) in the presence of 20 mg of the liver-specific transcriptional inhibitor D-(+)-galactos-amine (GalN, Sigma).

Isolation of Hepatic and Splenic T cells

Whole livers, liver draining lymph nodes (portal and celiac) and spleens were harvested from euthanised mice at indicated time points. Single cell suspensions were prepared by disruption of organs through a 100-μm mesh filter. Pooled immune cells were resuspended in 40% Percoll (GE Healthcare) and centrifuged at 300 x g for 20 min at room temperature. CD4+ and CD8+ T cells were isolated by

magnetic sorting, using negative selection Pan T Cell Isolation Kit II (Miltenyi Biotech). T cell enrichment was confirmed by FACS. Briefly, 1x10^6 cells were stained for 1 hour at 4°C in PBS supplemented with 2% FCS (Sigma-Aldrich) using fluorochrome-conjugated antibodies against: CD8 (PE; clone 53–6.7; BD Biosciences), CD4 (Pacific Blue; clone GK1.5 BD Biosciences), CD44 (FITC; clone IM7; BD Biosciences) and CD3 (PerCP; clone 1452C11; BD Biosciences). Data were acquired using a LSRFortessa Cell Analyzer (BD Biosciences) and analyzed with FlowJo Software (FlowJo LLC).

Cytokine Assays
Serum cytokines were determined using the Cytometric Bead Assay Flex System Kit (BD Bioscience) according to the manufacturer's instructions.

Western Blotting
Total liver protein lysates were prepared from 25 mg liver tissue that was homogenized in cell lysis buffer containing 20 mM Tris·HCl, pH 7.5, 135 mM NaCl, 1.5 mM Mg2Cl, 1 mM EGTA, 1% Triton X-100 (Sigma-Aldrich), 10% Glycerol (Ajax FineChem), EDTA-free protease inhibitor mixture tablets, and phosphatase inhibitor mixture tablets (Roche) using a tissue homogenizer (Tissue Lyser II; QIAGEN). Lysates (50 μg protein per lane) were separated using 4%–12% SDS/PAGE. Proteins were transferred onto nitrocellulose membranes and detected using primary and secondary antibodies. Antibodies used: hamster anti-TNFR1 (1:1,000; mab430; R&D Systems) and rabbit anti–β-actin (1:3,000; Cell Signaling Technology).

Immunofluorescence assay
Purified PbGFP-Luccon sporozoites were fixed with 4% paraformaldehyde / 0.0075% glutaraldehyde in 1x PBS at room temperature for 20 minutes, washed 3 times with 1x PBS and spotted on to slides at 25,000 sporozoites per slide. Slides were air-dried and then blocked in 3% BSA / 1x PBS, for 1 hour at room temperature. Mouse serum was diluted 1/500 with 1% BSA / 1x PBS and incubated on slides for 1 hour at room temperate. Slides were rinsed 3x times with 1x PBS and incubated with goat anti-mouse-A594 1/1000 in 1%BSA/ 1x PBS for 1 hour at room temperature. Slides were rinsed 3x times with 1x PBS, air-dried and mounted with Vecta Shield (Vector Laboratories, Burlingame, CA). Sporozoites were imaged using the tiling function on a Zeiss LiveCell AxioObserver with 100x objective.

Quantification and statistical analysis
Prism 7 software (GraphPad) was used to perform statistical tests and to determine sample size for experiments based on anticipated effect sizes. Groups (n = 3-14) were compared by unpaired two-tailed t tests for parametric data. Holm-Sidak correction was applied for multiple t tests. Log-rank (Mantel-Cox) test was used for analysis of time to event data. Non-parametric data was log-transformed for statistical analysis, or when this failed to normalize the data, Mann-Whitney tests were used. Data used are mean ± standard error of the mean (SEM).

Ethics Statement
All work with animals was approved by the Animal Ethics Committee of the Walter and Eliza Hall Institute of Medical Research.

DATA AND CODE AVAILABILITY

This study did not generate any unique datasets or code.